International Journal of Power Electronics and Drive System (IJPEDS)
Vol. 16, No. 2, June 2025, pp. 840∼850
ISSN: 2088-8694, DOI: 10.11591/ijpeds.v16.i2.pp840-850

Single-neuron adaptive double-power super-twisting sliding mode control for induction motor

Siham Mencou, Majid Ben Yakhlef, El Bachir Tazi
Engineering Sciences Laboratory, Polydisciplinary Faculty of Taza, Sidi Mohamed Ben Abdellah University, Fez, Morocco

Article Info

Article history:

Received Oct 19, 2024
Revised Apr 9, 2025
Accepted May 6, 2025

Keywords:

Direct torque control
Double-power-super-twisting algorithm
Induction motor
Single-neuron adaptive control
Sliding mode control

ABSTRACT

Direct torque control is a widely used control method for induction motors because it offers rapid dynamic response and relatively simple implementation. However, it presents high torque and flux ripples and variable switching frequencies. To overcome these constraints, the double-power super-twisting sliding mode (DPSTSM) control approach has been proposed, integrating the advantages of the super-twisting algorithm designed to reduce chattering with those of the double power convergence law aimed to improve system speed and dynamic quality. However, the optimal tuning of the sliding mode gains of the double-power super-twisting sliding mode controller represents a considerable challenge. To address this issue, we proposed an improvement to the DPSTSM algorithm through the integration of a single-neuron adaptive algorithm. The single-neuron adaptive double-power super-twisting sliding mode control approach aims to dynamically adjust the controller gains, while delivering superior performance in terms of chattering reduction, improved dynamic response, and enhanced robustness to load disturbances. A detailed investigation was carried out via MATLAB/Simulink simulations to determine the effectiveness of the proposed control strategy.

Corresponding Author:

Siham Mencou
Engineering Sciences Laboratory, Polydisciplinary Faculty of Taza, Sidi Mohamed Ben Abdellah University
Fez, Morocco
Email: siham.mencou@usmba.ac.ma

1. INTRODUCTION

Induction motors (IM) have attained considerable acclaim in industrial and transportation sectors due to their cost-effectiveness, durability, and minimal maintenance requirements [1]–[4]. It accounts for more than 60% of the total electrical energy consumption within the industrial sectors of developed countries [5]. Analyses predict that the induction motor industry is expected to achieve a compound annual growth rate of 3.72% from 2019 through 2028, culminating in a market worth $20,316 million by the year 2028 [6].

However, these motors pose distinct challenges regarding control owing to their non-linear dynamics and susceptibility to parameter variations [7]–[9]. Their control requires advanced strategies to ensure optimal operational performance. Direct torque control (DTC) is frequently employed in induction machine applications, as it provides a swift dynamic response and facilitates straightforward implementation [10], [11]. However, traditional DTC exhibits notable drawbacks, including high torque and flux ripples alongside variable switching frequencies [12]–[14]. This variability stems from its hysteresis-based control system, which triggers switching at irregular intervals [15]. These issues detrimentally influence system performance, induce mechanical vibrations, and increase component wear.

In order to address these limitations, the double-power super-twisting sliding mode (DPSTSM) algorithm has been introduced [16], integrating the beneficial characteristics of the super-twisting algorithm (STA), which mitigates the chattering phenomenon [17]–[20], alongside those of the double power sliding mode reaching law (DPSMRL), which enhances both the reaching speed and the dynamic quality of the system [21], [22]. As delineated in the study [16], the efficacy of the proposed controller is assessed within the framework of DTC for induction motor-driven electric vehicles, and is juxtaposed with the performance of proportional-integral (PI), fuzzy logic, and super-twisting sliding mode controllers. The results indicate that the DPSTSM control enhances the robustness of the control system and substantially mitigates chattering, whilst preserving elevated dynamic performance. However, since the operating conditions of IMs vary considerably due to various factors such as load changes, temperature variations and component ageing, determining the optimum sliding-mode gains of the DPSTSM controller is a major challenge in maintaining optimum performance. Incorrect setting of these parameters can lead to degraded dynamic performance and even system instability, which is unacceptable in critical industrial environments.

In response to the aforementioned challenges, this paper introduces an enhancement of the DPSTSM algorithm that incorporates an adaptive single-neuron approach. The single-neuron adaptive method provides an effective solution for dynamically adjusting controller parameters. This methodology leverages the learning and adaptive proficiencies inherent in neural networks, even when represented in a simplified architecture comprising a single neuron, to fine-tune controller parameters in alignment with fluctuations in operational circumstances without unnecessarily complicating the controller [23]–[25]. In contrast to conventional multi-layer neural networks, the utilization of a single neuron diminishes computational complexity and promotes practical applicability, while simultaneously preserving a robust capacity for adaptation [26], [27].

Recent researches suggest that applying artificial intelligence strategies, like neural networks and adaptive algorithms, can bring about noteworthy improvements in dynamic response and stability indicators. In [28]–[31], researchers employed neural adaptive control mechanisms to calibrate the three essential PID control parameters, specifically the proportional, integral, and derivative coefficients, thereby addressing the challenge posed by the complex gain parametrization inherent in traditional PID controllers. The findings demonstrated that neural adaptive control significantly elevates the performance of conventional PID control systems, providing augmented robustness, stability, and dynamic operational efficacy.

By incorporating a single adaptive neuron within the framework of the DPSTSM algorithm, our objective is to enhance the robustness and dynamic responsiveness of the system while concurrently mitigating torque and flux ripples. This paper is organized as follows: The second section elucidates the principles underlying the single-neuron adaptive methodology and its integration into the DPSTSM controller tailored for the direct torque control approach. The third section presents the methodologies used for system modeling and simulation. Subsequently, we present the simulation results and a detailed performance analysis of the proposed system. At the end of the study, we conclude by summarizing the main contributions.

2. SINGLE-NEURON ADAPTIVE DOUBLE-POWER SUPER-TWISTING CONTROLLER DESIGN

2.1. Double-power super-twisting controller

The DPSTSM algorithm has been designed to enhance the performance of the STA algorithm by exploiting the properties of the DPSMRL [16]. The main idea is to replace the switching mechanism of the STA with that of DPSMRL. The fundamental structure of this algorithm is delineated as (1).

$$\begin{cases} \dfrac{dx_1}{dt} = -k_1\phi_1\left(x_1\right) + x_2 + \varphi_1\left(x_1, t\right) \\ \dfrac{dx_2}{dt} = -k_2\phi_2\left(x_1\right) + \varphi_2\left(x_2, t\right) \end{cases} \tag{1}$$

With:

$$\begin{cases} \phi_1(x) = |x|^{1/2}\ \operatorname{sign}(x) + \lambda|x|^{3/2}\ \operatorname{sign}(x) \\ \phi_2(x) = \left(\phi_1^2(x)\right)' = 2\phi_1(x)\cdot\phi_1(x)' = \operatorname{sign}(x) + 4\lambda|x|\operatorname{sign}(x) + \dfrac{3}{2}\lambda^2|x|^2\operatorname{sign}(x) \end{cases} \quad ; \quad \lambda \geq 0$$

where k_1 and k_2 are sliding mode gains coefficients. If for constants $\delta_1 \geq 0$ and $\xi_1 = \frac{1}{\phi_1' \ (x_1)}$ as (2).

$$|\varphi_1| \leq \delta_1 \, |\zeta_1| \quad and \quad \varphi_2 = 0 \ \ ; \ \forall t \geq 0 \tag{2}$$

The system will approach the equilibrium point $x(0,0)$ within a finite temporal duration, provided that the sliding mode gains k_1 and k_2 satisfy the conditions as (3) [16].

$$\begin{cases} k_1 > 2\delta_1 \\ k_2 > k_1 \frac{5\delta_1 k_1 + 4\delta_1^2}{2(k_1 - 2\delta_1)} \end{cases} \tag{3}$$

As detailed in [16], the DPSTSM control command is expressed as (4).

$$u(t) = -k_1 \left(\left(|s(t)|^{\frac{1}{2}} + \lambda |s(t)|^{\frac{3}{2}} \right) \operatorname{sign}(s(t)) \right) - \int k_2 \left(\left(1 + 4\lambda |s(t)| + \frac{3}{2} \lambda^2 |s(t)|^2 \right) \operatorname{sign}(s(t)) \right) \tag{4}$$

With $s(t)$ the sliding variable.

Although the controller ensures system stability as long as the gains satisfy the stability conditions as (3), these conditions allow a wide range of values, which makes it difficult to calculate the specific gain values k_1 and k_2. This causes problems for the design of optimal controller parameters.

To solve this problem, we designed a single-neuron adaptive double-power super-twisting sliding mode (SNA-DPSTSM) controller for adjusting the gain of the DPSTSM controller in real-time. This approach merges the benefits of the single-neuron adaptive control method, known for its simplicity and adaptability, with the principles of DPSTSM control theory. The specific steps involved in designing this control algorithm are described in 2.2.

2.2. Single-neuron adaptive double-power super-twisting sliding mode controller design

Figure 1 shows the overall block diagram of the SNA-DPSTSM controller approach proposed in this study, where the control $u(k)$ is dynamically adjusted as a function of the sliding variable $s(k)$. Since the single-neuron controller operates using a numerical control, it is essential to discretize the DPSTSM control command described in (4). We used the direct finite difference method for this discretization. This approach allowed us to transform the continuous controller into an incremental controller, adapted for a numerical environment.

The discrimination of $u(t)$ is given by (5):

$$\begin{aligned} u(k) = k_1' |s(k)|^{\frac{1}{2}} \operatorname{sign}(s(k)) + k_2' |s(k)|^{\frac{3}{2}} \operatorname{sign}(s(k)) + k_3' \sum_{i=0}^{k} \operatorname{sign}(s(i)) \\ + k_4' \sum_{i=0}^{k} |s(i)| \operatorname{sign}(s(i)) + k_5' \sum_{i=0}^{k} |s(i)|^2 \operatorname{sign}(s(i)) \end{aligned} \tag{5}$$

With (6):

$$\begin{cases} k_1' = k_1 \\ k_2' = k_1 \lambda \\ k_3' = k_2 \\ k_4' = 4 k_2 \lambda \\ k_5' = \frac{3}{2} k_2 \lambda^2 \end{cases} \tag{6}$$

The incremental controller is given by (7).

$$\begin{aligned} \Delta u(k) &= u(k) - u(k-1) \\ &= k_1' \left(|s(k)|^{\frac{1}{2}} \operatorname{sign}(s(k)) - |s(k-1)|^{\frac{1}{2}} \operatorname{sign}(s(k-1)) \right) \\ &+ k_2' \left(|s(k)|^{\frac{3}{2}} \operatorname{sign}(s(k)) - |s(k-1)|^{\frac{3}{2}} \operatorname{sign}(s(k-1)) \right) \\ &+ k_3' \operatorname{sign}(s(k)) + k_4' |s(k)| \operatorname{sgn}(s(k)) + k_5' |s(k)|^2 \operatorname{sign}(s(k)) \end{aligned} \tag{7}$$

We define the set variables as (8).

$$\begin{cases} v_1(k) = |s(k)|^{\frac{1}{2}}\,\mathrm{sign}(s(k)) - |s(k-1)|^{\frac{1}{2}}\,\mathrm{sign}(s(k-1)) \\ v_2(k) = |s(k)|^{\frac{3}{2}}\,\mathrm{sign}(s(k)) - |s(k-1)|^{\frac{3}{2}}\,\mathrm{sign}(s(k-1)) \\ v_3(k) = \mathrm{sign}(s(k)) \\ v_4(k) = |s(k)|\,\mathrm{sign}(s(k)) \\ v_5(k) = |s(k)|^2\,\mathrm{sign}(s(k)) \end{cases} \tag{8}$$

These state variables are the inputs to our single neuron, as shown in Figure 1. To each input variable $v_i(k)$, we assign a weighting factor $\omega_i(k)$. Based on the input variables and the weighting factors, the neuron calculates the incremental controller as in (9).

$$\Delta u(k) = K\sum_{i=1}^{5}\omega_i(k)v_i(k) \tag{9}$$

Where K is the neuron gain coefficient $K > 0$, and $k_i' = K\omega_i(k)$ for $i = 1, \ldots, 5$.

Adaptive learning was chosen for the adjustment of the weighting factors because it allows the weights to be dynamically modified in response to variations in the error. This approach guarantees a faster and more stable convergence of the model. We define the objective function J as a measure of the squared error $J = \frac{s(k)^2}{2}$, given as (10).

$$\Delta\omega_i(k) = -\eta_i\frac{\partial J}{\partial\omega_i} \tag{10}$$

Using improved Hebb-supervised learning, we obtain (11).

$$\Delta\omega_i(k) = \eta_i s(k)u(k-1)(2s(k) - s(k-1)) \tag{11}$$

To avoid uncontrolled weight gain, the output is obtained after normalizing the weighting factors as in (12).

$$\Delta u(k) = K\sum_{i=1}^{5}\omega_i'(k)v_i(k) \quad \text{with: } \omega_i'(k) = \frac{\omega_i(k)}{\sum_{i=1}^{5}\omega_i(k)} \tag{12}$$

Whereas in (13).

$$\omega_i(k) = \omega_i(k-1) - \eta_i s(k)u(k-1)(2s(k) - s(k-1)) \tag{13}$$

The SNA_DPSTSM control command will be expressed as (14).

$$u(k) = u(k-1) + K\sum_{i=1}^{5}\omega_i'(k)v_i(k) \tag{14}$$

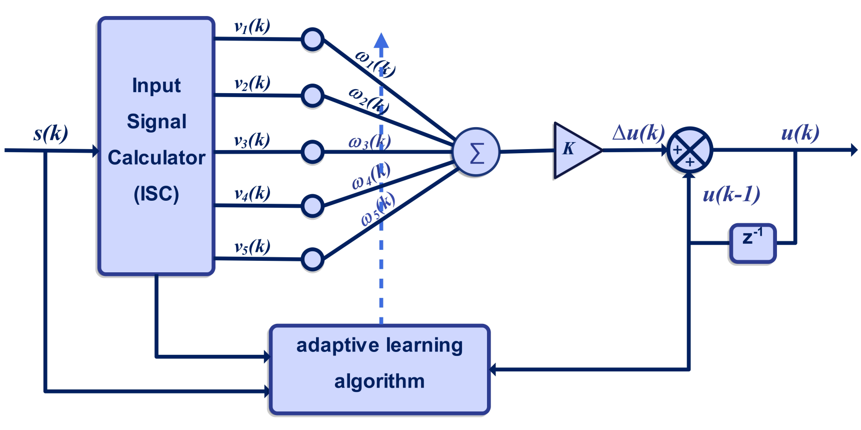

Figure 1. Block diagram of SNA-DPSTSM controller

3. SYSTEM MODELING AND SIMULATION METHODOLOGY

3.1. Integration the SNA_DPSTSM controller in DTC control

In order to verify the accuracy and efficiency of the proposed SNA_DPSTSM controller, we tested it in the context of DTC control of an induction motor [16]. Figure 2 shows the block diagram of the DTC control of an IM based on a SNA_DPSTSM controller. This control algorithm is integrated into the closed-loop speed control. The SNA_DPSTSM controller calculates the control command u(k) based on the speed error. The reference torque T^*_{em} is calculated according to (15) [16].

$$T^*_{em} = f_v \omega^*_m + J\omega^*_m + T_L - Ju \tag{15}$$

3.2. System modeling and simulation methodology

To test in detail the performances of the SNA_DPSTSM proposed controller, simulations were performed using MATLAB/Simulink. Figure 3 shows the simulation model structure of the induction motor (IM) controlled by the DTC strategy based on the SNA-DPSTSM speed controller. The detailed modeling of the DTC control of IM is presented in [16].

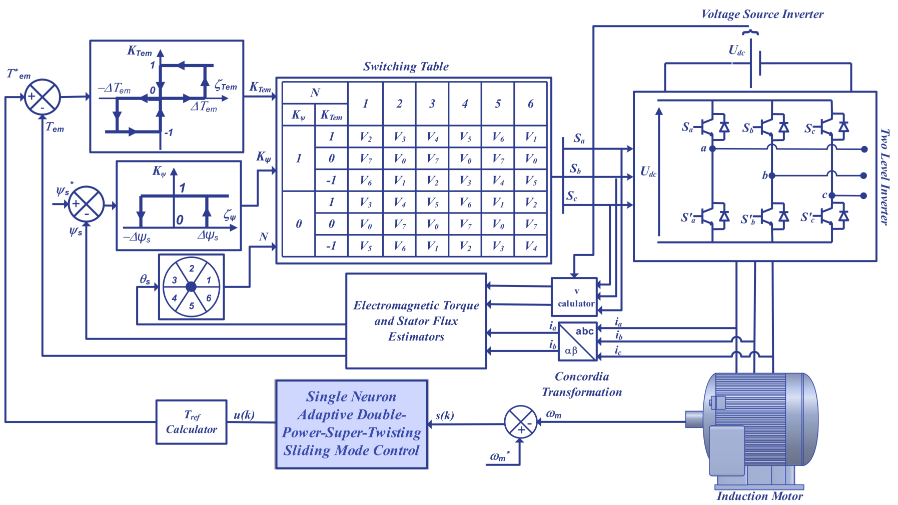

Figure 2. Block diagram DTC control of IM based on a SNA_DPSTSM controller

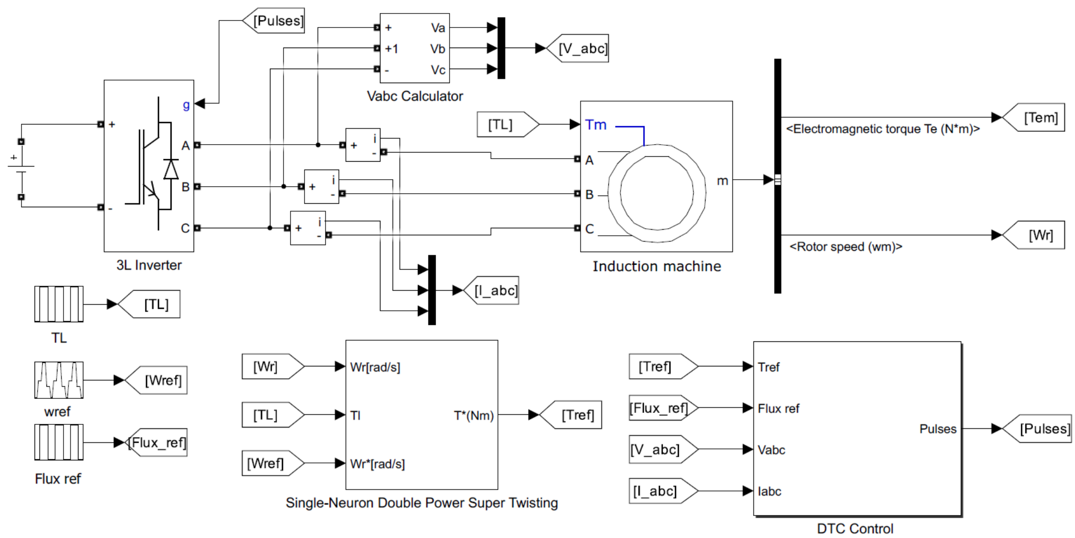

Figure 3. General system modeling structure of DTC based on SNA_DPSTSM controller

4. SIMULATIONS AND RESULTS

In this section, we delineate the simulation outcomes acquired to assess and scrutinize the efficacy of the proposed SNA_DPSTSM controller. These performance metrics are evaluated alongside those of the DPSTSM and PI controllers [16]. For the simulation, we chose a 4 KW induction motor with two pairs of poles, whose parameters are summarized in Table 1. The PI and DPSTSM controller parameters used for the simulation were $K_p = 8$, $K_i = 32$, $K_1 = 35$, $K_2 = 15$, and $\lambda = 3/2$, which were optimized using the trial-and-error approach. The neuron's gain coefficient was set to $K = 25$, and the initial values of the weighting factors were 0.1.

Table 1. Induction machine parameters

Parameter	Value	Parameter	Value
Nominal power	4 kW	Stator resistance (R_s)	1.405 Ω
Nominal voltage	400 V	Rotor resistance (R_r)	1.395 Ω
Frequency	50 Hz	Stator inductance (L_s)	0.005839 H
Inertia (J)	0.0131 $kg.m^2$	Rotor inductance (L_r)	0.005839 H
Friction factor (f_v)	0.002985 N.m.s	Mutual inductance (L_m)	0.1722 H

Firstly, we examine the controller's responses to a reference speed setpoint of 75 rad/s applied at 0.05 s and a load torque of 28 Nm introduced at 0.3 s. The reference value of the stator flux module is set to 1.1 Wb. Simulation results are presented in Figure 4. The speed response of the three controllers, illustrated in Figure 4(a), shows that, under the action of the PI control, the motor speed follows the reference value with an overshoot of 5.84% and a steady-state error of 0.12 rad/s in the absence of load and 0.43 rad/s when load is applied. On the other hand, under the command of the DPSTSM controller, the motor operates without overshoot, but has a relatively longer regulation time: 0.15 s for speed variation and 0.03 s for torque variation. In contrast, the SNA_DPSTSM proposed controller demonstrated superior performance in terms of both response time and steady-state error. Under the control of the SNA_DPSTSM controller, the motor accurately follows the setpoint signal without displacement, with a very fast response time of 12 ms for speed variation and just 2 ms for torque variation adjustment.

As shown in Figures 4(b) and 4(c), the integration of the single-neuron adaptive algorithm into the DPSTSM has significantly reduced stator flux and torque ripples. This approach decreases steady-state torque ripples to 14.64%, compared with 15.88% for the DPSTSM and 17.83% for the PI. In addition, the proposed SNA-DPSTSM controller minimizes flux fluctuations by 60% compared with the DPSTSM. To further assess the effectiveness of the proposed controller, we test its robustness and stability under more demanding operating conditions. We apply a reference speed setpoint varying between 0 rad/s and 157 rad/s over a period of 22 s, with a rectangular load torque signal of 14 Nm amplitude applied between 5 s and 17 s.

Variations of the controller parameters k_1, k_2, k_3, k_4 and k_5 are shown in Figures 5(a)-5(e). The results clearly demonstrate the ability of the proposed single-neuron adaptive algorithm to dynamically and optimally adjust these parameters according to the operating conditions of the system. Figure 5(f), which illustrates the variation of the objective function J, shows that the latter converges to 0 in steady state. This shows that the proposed algorithm succeeds in efficiently minimizing the error.

The simulation results, presented in Figure 6, illustrate that under the action of the SNA-DPSTSM controller, the motor speed follows the reference signal quickly and efficiently, without overshoot, while maintaining overall system stability. Unlike the PI and DPSTSM controllers, the adaptive neural network controller showed robustness to load disturbances and the ability to adapt dynamically to changing operating conditions. In addition, a comparative study was conducted using minimization criteria, specifically the integral square error (ISE) and the integral absolute error (IAE). These two statistical parameters are commonly used in control systems to evaluate and compare the performance of closed-loop systems.

According to the values of the evaluation parameters shown in Table 2, the PI controller showed the least satisfactory behavior compared to the other controllers, with high values for IAE (0.410) and ISE (2.340). In contrast, the DPSTSM controller showed superior performance, displaying lower values for the statistical parameters (IAE: 0.367 and ISE: 0.798). However, the proposed SNA_DPSTSM controller showed the most promising results compared with the other controllers, with an IAE of 0.021 and an ISE of 0.177. The use of an SNA controller showed exceptional ability to minimize error over time.

(a)

(b)

(c)

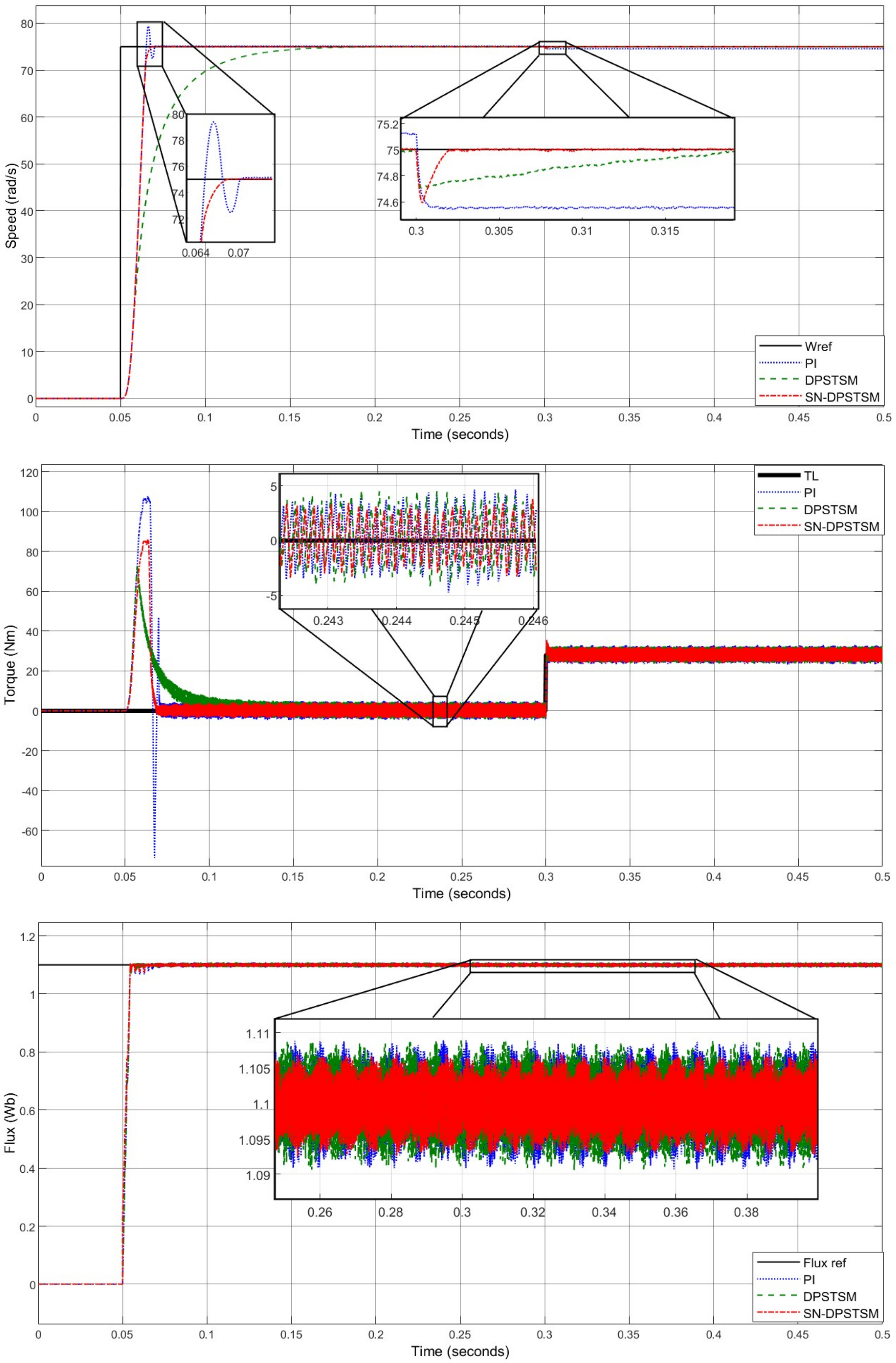

Figure 4. Simulation results of the PI, DPSTSM, and SNA_DPSTSM controllers: (a) rotor speed, (b) electromagnetic torque, and (c) stator flux

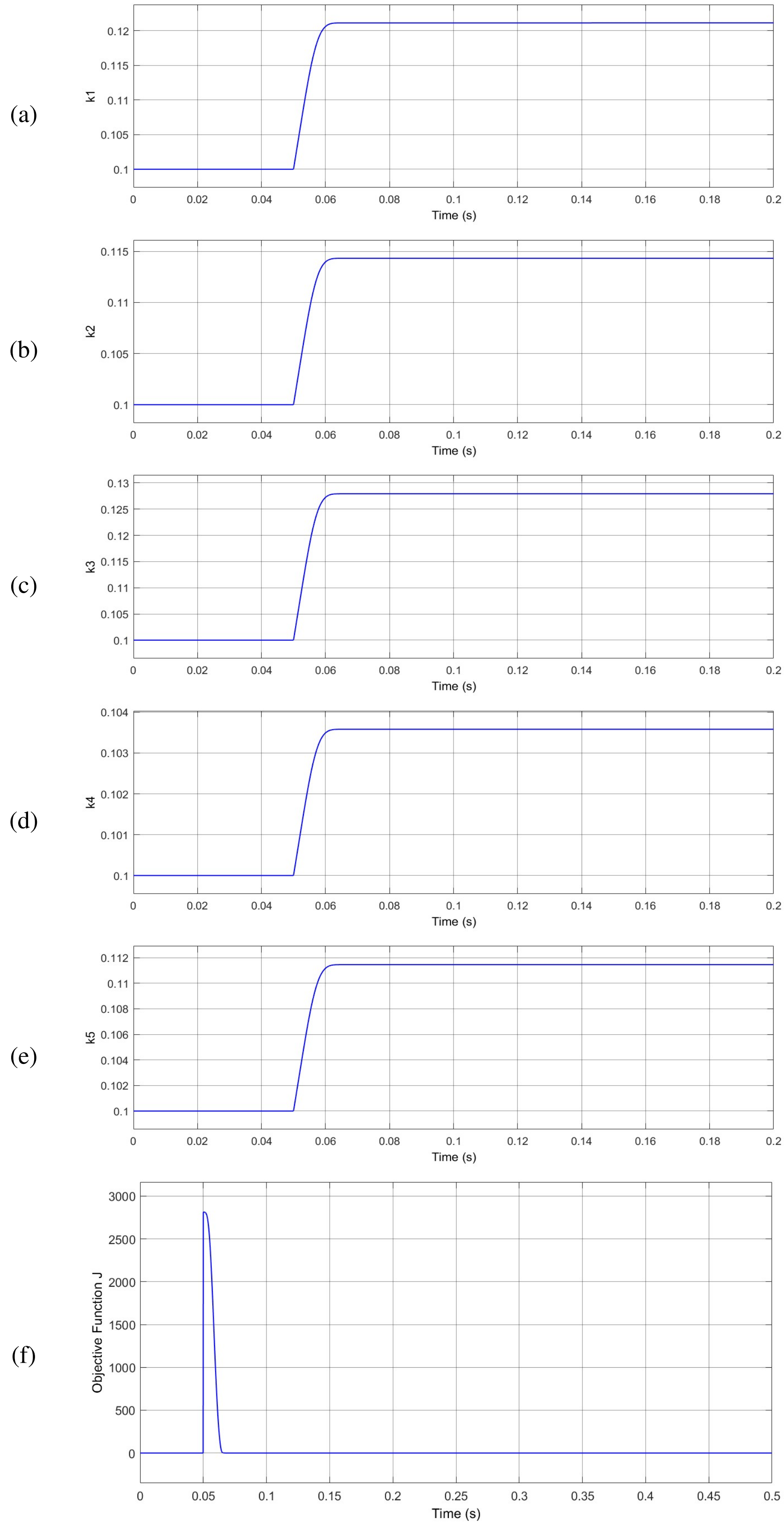

Figure 5. Variations of the controller parameters: (a) k_1, (b) k_2, (c) k_3, (d) k_4, (e) k_5, and (f) the objective function J

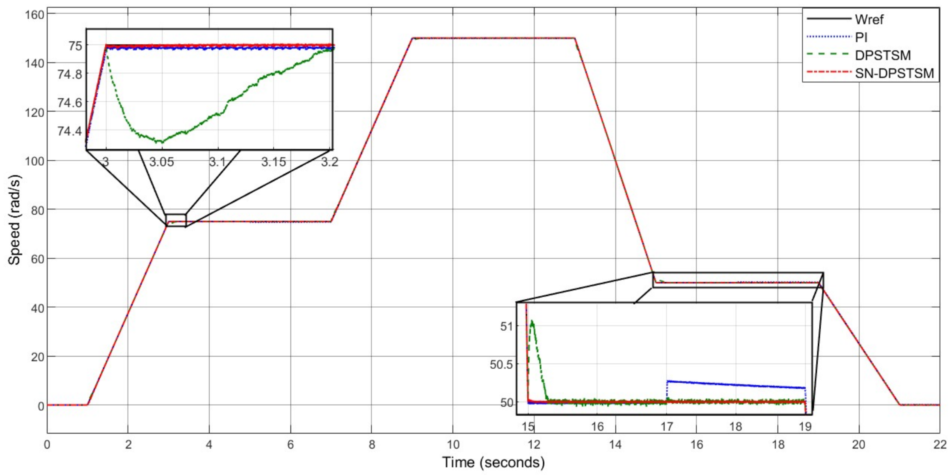

Figure 6. Rotor speed response for a speed variation from 0 rad/s to 157 rad/s

Table 2. Evaluation of ISE end IAE parameters

Parameter	PI	DPSTSM	SNA-DPSTSM
ISE	0.410	0.367	0.021
IAE	2.340	0.798	0.177

These results highlight the improvements brought by the integration of the single-neuron adaptive algorithm into the DPSTSM controller in terms of self-adjustment of the controller, reduced chattering, improved dynamic response, and robustness to variations in system parameters. This guarantees more efficient and reliable control, even under variable operating conditions, making it an ideal solution for applications requiring high precision and increased robustness, such as motor control in electric vehicles or other demanding industrial systems.

The findings elucidate the enhancements facilitated by the incorporation of the single-neuron adaptive algorithm into the DPSTSM controller, particularly regarding the self-adjustment of controller parameters, the mitigation of chattering, the enhancement of dynamic response, and the resilience to fluctuations in system parameters. This ensures a more efficacious and dependable control mechanism, even in the face of variable operational conditions, thereby rendering it an optimal solution for applications necessitating high precision and augmented robustness, such as motor control within electric vehicles or other high-demand industrial systems.

5. CONCLUSION

This paper introduces an enhancement of the DPSTSM algorithm through the incorporation of a single-neuron adaptive algorithm, specifically designed to address the issue of optimal controller gain adjustment. Simulation results showed that the single-neuron adaptive controller facilitates dynamic and optimal adjustment of control parameters under different operating conditions. The proposed SNA_DPSTSM controller has exhibited superior performance compared to both the DPSTSM and PI controllers by delivering prompt and precise responses to setpoint and load variations, significantly mitigating the chattering phenomenon, reducing torque and flux ripples and enhancing resilience against disturbances and fluctuations in operational conditions. Furthermore, the inherent simplicity of the single-neuron algorithm promotes the practical deployment of the controller, while concurrently diminishing the computational complexity in relation to conventional multi-layer neural networks. These advancements render the SNA_DPSTSM controller exceptionally well-suited for applications necessitating high levels of precision and robustness, such as motor control in electric vehicles and in rigorous industrial environments.

FUNDING INFORMATION

This research did not receive any specific grant from funding agencies in the public, commercial, or not-for-profit sectors.

AUTHOR CONTRIBUTIONS STATEMENT

This journal uses the Contributor Roles Taxonomy (CRediT) to recognize individual author contributions, reduce authorship disputes, and facilitate collaboration.

Name of Author	C	M	So	Va	Fo	I	R	D	O	E	Vi	Su	P	Fu
Siham Mencou	✓	✓	✓	✓	✓	✓	✓	✓	✓		✓		✓	
Majid Ben Yakhlef	✓			✓						✓		✓		
El Bachir Tazi	✓			✓						✓		✓		

C : **C**onceptualization
M : **M**ethodology
So : **So**ftware
Va : **Va**lidation
Fo : **Fo**rmal Analysis
I : **I**nvestigation
R : **R**esources
D : **D**ata Curation
O : Writing - **O**riginal Draft
E : Writing - Review & **E**diting
Vi : **Vi**sualization
Su : **Su**pervision
P : **P**roject Administration
Fu : **Fu**nding Acquisition

CONFLICT OF INTEREST STATEMENT

Authors state no conflict of interest.

DATA AVAILABILITY

The authors confirm that the data supporting the findings of this study are available within the article and/or its supplementary materials.

REFERENCES

[1] P. Dinolova, V. Ruseva, and O. Dinolov, "Energy efficiency of induction motor drives: State of the art, analysis and recommendations," *Energies*, vol. 16, no. 20, p. 7136, 2023, doi: 10.3390/en16207136.

[2] M. L. De Klerk and A. K. Saha, "A comprehensive review of advanced traction motor control techniques suitable for electric vehicle applications," *IEEE Access*, vol. 9, pp. 125080–125108, 2021, doi: 10.1109/ACCESS.2021.3110736.

[3] R. Chen and T. Tong, "Induction motors and permanent magnet motors in electric vehicles: Characteristics and development trends," in *2023 International Conference on Internet of Things, Robotics and Distributed Computing (ICIRDC)*, pp. 221–224, 2023, doi: 10.1109/icirdc62824.2023.00046.

[4] O. E. M. Youssef, M. G. Hussien, and A. El-Wahab Hassan, "A robust regenerative-braking control of induction motors for EVs applications," *International Transactions on Electrical Energy Systems*, vol. 2024, no. 1, 2024, doi: 10.1155/2024/5526545.

[5] M. G. Simões, "A concise history of induction motor drives—Part 1 [History]," *IEEE Electrification Magazine*, vol. 11, no. 2, pp. 5–11, 2023, doi: 10.1109/mele.2023.3264888.

[6] Triton Market Research, "Global induction motors market 2019–2028: Market by type, application, and geography," Automotive & Transportation — Automotive Components. [Online]. Available: https://www.tritonmarketresearch.com/reports/induction-motors-market

[7] A. El-Shahat, *Induction motors: recent advances, new perspectives and applications*, IntechOpen, 2023, doi: 10.5772/intechopen.104031.

[8] P. Thirugnanam, "Advances, new perspectives and applications in induction motors," in *Induction Motors: Recent Advances, New Perspectives and Applications*, IntechOpen, 2023, doi: 10.5772/intechopen.1001583.

[9] M. V. Sarin, A. Chitra, P. Sanjeevikumar, and A. Venkadesan, "Induction motor control schemes for hybrid electric vehicles/electric vehicles," in *Artificial Intelligent Techniques for Electric and Hybrid Electric Vehicles*, pp. 165–178, 2020, doi: 10.1002/9781119682035.ch9.

[10] M. Aktas, K. Awaili, M. Ehsani, and A. Arisoy, "Direct torque control versus indirect field-oriented control of induction motors for electric vehicle applications," *Engineering Science and Technology, an International Journal*, vol. 23, no. 5, pp. 1134–1143, 2020, doi: 10.1016/j.jestch.2020.04.002.

[11] R. H. Kumar, A. Iqbal, and N. C. Lenin, "Review of recent advancements of direct torque control in induction motor drives–a decade of progress," *IET Power Electronics*, vol. 11, no. 1, pp. 1–15, 2018, doi: 10.1049/iet-pel.2017.0252.

[12] S. Mencou, M. B. Yakhlef, and E. B. Tazi, "Advanced torque and speed control techniques for induction motor drives: A review," in *2022 2nd International Conference on Innovative Research in Applied Science, Engineering and Technology (IRASET)*, pp. 1–9, 2022, doi: 10.1109/IRASET52964.2022.9738368.

[13] J. Jeyashanthi and J. B. Banu, "Performance analysis of DTC-IM drive using various control algorithms," in *Futuristic Projects in Energy and Automation Sectors*, pp. 191, 2023, doi: 10.2174/9789815080537123010014.

[14] N. El Ouanjli *et al.*, "Modern improvement techniques of direct torque control for induction motor drives–a review," *Protection and Control of Modern Power Systems*, vol. 4, no. 2, pp. 1–12, 2019, doi: 10.1186/s41601-019-0125-5.

[15] T. Sutikno, N. R. N. Idris, and A. Jidin, "A review of direct torque control of induction motors for sustainable reliability and energy efficient drives," *Renewable and Sustainable Energy Reviews*, vol. 32, pp. 548–558, 2014, doi: 10.1016/j.rser.2014.01.040

[16] S. Mencou, M. B. Yakhelf, and E. Tazi, "Direct torque control of induction motor based on double-power-super-twisting sliding mode speed control for electric vehicle applications," *International Journal of Power Electronics and Drive System (IJPEDS)*, vol. 15, no. 3, pp. 1399–1409, 2024, doi: 10.11591/ijpeds.v15.i3.pp1399-1409.

[17] R. I. Verdés, A. F. de Loza, L. T. Aguilar, I. Castillo, and L. Freidovich, "Accurate position regulation of an electro-hydraulic actuator via uncertainty compensation-based controller," in *Emerging Trends in Sliding Mode Control*, pp. 279–303, 2021, doi: 10.1007/978-3-030-65702-3_11.

[18] A. Levant, "Sliding order and sliding accuracy in sliding mode control," *International Journal of Control*, vol. 58, no. 6, pp. 1247–1263, 1993, doi: 10.1080/00207179308923053.

[19] A. Ammar, "Second-order sliding mode-direct torque control and load torque estimation for sensorless MRAS-based induction machine," *Journal of System and Control Engineering*, vol. 235, no. 1, pp. 15–29, 2021, doi: 10.1177/0959651820935694.

[20] R. Sadeghi, S. M. Madani, M. Ataei, M. R. Agha Kashkooli, and S. Ademi, "Super-twisting sliding mode direct power control of a brushless doubly fed induction generator," *IEEE Transactions on Industrial Electronics*, vol. 65, no. 11, pp. 9147–9156, 2018, doi: 10.1109/TIE.2018.2818672.

[21] M. Tao, Q. Chen, X. He, and M. Sun, "Adaptive fixed-time fault-tolerant control for rigid spacecraft using a double power reaching law," *International Journal of Robust and Nonlinear Control*, vol. 29, no. 12, pp. 4022–4040, 2019, doi: 10.1002/rnc.4593.

[22] H. J. Li and Y. L. Cai, "Sliding mode control with double power reaching law," *Control Decision*, vol. 31, no. 3, pp. 498–502, 2016, doi: 10.13195/j.kzyjc.2014.1908.

[23] L. Cheng, Z. Wang, F. Jiang, and J. Li, "Adaptive neural network control of nonlinear systems with unknown dynamics," *Advances in Space Research*, vol. 67, no. 3, pp. 1114–1123, 2021, doi: 10.1016/j.asr.2020.10.052.

[24] W. Tang, L. Wang, J. Gu, and Y. Gu, "Single neural adaptive PID control for small UAV micro-turbojet engine," *Sensors*, vol. 20, no. 2, p. 345, 2020, doi: 10.3390/s20020345.

[25] S. Morris, "A neuro-sliding mode controller for STATCOM," *Electric Power Components and Systems*, vol. 32, no. 2, pp. 131–147, 2004, doi: 10.1080/15325000490195853.

[26] C. Napole, O. Barambones, I. Calvo, and J. Velasco, "Feedforward compensation analysis of piezoelectric actuators using artificial neural networks with conventional PID controller and single-neuron PID based on Hebb learning rules," *Energies*, vol. 13, no. 15, p. 3929, 2020, doi: 10.3390/en13153929.

[27] Y. Qin and H. Duan, "Single-neuron adaptive hysteresis compensation of piezoelectric actuator based on Hebb learning rules," *Micromachines*, vol. 11, no. 1, p. 84, 2020, doi: 10.3390/mi11010084.

[28] X.-t. Wang, X.-c. Wang, and K.-w. Liu, "Adaptive PID control of coal feeder based on single neuron," in *Proceedings of the 2019 International Conference on Modeling, Analysis, Simulation Technologies and Applications (MASTA 2019)*, pp. 347–352, 2019, doi: 10.2991/masta-19.2019.58.

[29] J. Hernandez-Barragan, J. D. Rios, A. Y. Alanis, C. Lopes-Franco, and J. Gomez-Avila, "Adaptive single neuron anti-windup PID controller based on the extended Kalman filter algorithm," *Electronics*, vol. 9, no. 4, p. 636, 2020, doi: 10.3390/electronics9040636.

[30] L. Yu, J. G. Lim, and S. Fei, "An improved single neuron self-adaptive PID control scheme of superheated steam temperature control system," *International Journal of System Control and Information Processing*, vol. 2, no. 1, 2017, doi: 10.1504/IJSCIP.2017.084253.

[31] Y. Zhang, P. Li, and W. Wu, "Single neuron PID sliding mode parallel compound control for alternating current servo system," *Procedia Engineering*, vol. 29, pp. 2055–2061, 2012, doi: 10.1016/j.proeng.2012.01.261.

BIOGRAPHIES OF AUTHORS

Siham Mencou was born in 1996 in Boulemane, Morocco. She obtained her engineering master's degree in electromechanics in 2019 from the National School of Mines in Rabat, Morocco. Currently, she is actively pursuing her Ph.D. at the Laboratory of Engineering Sciences, Polydisciplinary Faculty of Taza, Sidi Mohamed Ben Abdellah University, Fez, Morocco. Her research focuses on artificial intelligence, control systems, and electric vehicle drive systems. She can be contacted at email: siham.mencou@usmba.ac.ma.

Majid Ben Yakhlef defended his doctoral thesis in computer science and automation at the University Sidi Mohamed Ben Abdellah (USMBA), Morocco. He was recruited in 2007 as a lecturer at the Faculty of Taza; he defended his HDR in 2012 following the research work he carried out at the LIMAO laboratory. Ben Yakhlef does his research in computer engineering, control systems engineering, and artificial intelligence. Currently a member of the Engineering Sciences Laboratory. In recent years, his work has shifted towards data science. He can be contacted at email: majid.benyakhlef@usmba.ac.ma.

El Bachir Tazi graduated in electronic engineering from ENSET Mohammedia, Morocco, in 1992. He obtained his DEA and DES in automatic control and signal processing, as well as his PhD in computer science from the Faculty of Sciences of Sidi Mohammed Ben Abdellah University (USMBA) in Fez, Morocco, in 1995, 1999, and 2012, respectively. He is currently a member of the Engineering Sciences Laboratory and a full professor at the Polydisciplinary Faculty of Taza, USMBA University. His research focuses on the applications of automatic speaker recognition systems and automatic control systems based on artificial intelligence techniques. He can be contacted at email: elbachir.tazi@usmba.ac.ma